

Radial Correlation Measurements at TEXTOR

A.Krämer-Flecken¹, S. Soldatov², T. Zhang¹ and the TEXTOR–Team

¹ *Institute for Energy Research – Plasma Physics, Forschungszentrum Jülich, EURATOM Association-FZJ, Trilateral Euregio Cluster, D–52425 Jülich*

² *Department of Applied Physics, Ghent University, Rozier 44, 9000 Gent Belgium*

Hardware Upgrade and Correlation Combinations

During the last year the reflectometer system at TEXTOR has been upgraded. A third antennae array in the equatorial plane and at a different toroidal position has been installed, which is $\Delta\phi = 112^\circ$ apart from the top antennae and $\Delta\phi = 90^\circ$ apart from the midplane antennae array. It consists of one launcher and two poloidally spaced receiving antennae. The whole array and the waveguide in the vessel allow the measurement of O– and X–mode polarization. In X–mode polarization fluctuation and rotation measurements up to a local electron density of $n_e = 5 \times 10^{19} \text{ m}^{-3}$ are possible.

The recently installed second millimeter wave generator consists of two voltage controlled oscillators. The oscillators are phase locked and operate at $\Delta f = f_1 - f_2 = 20 \text{ MHz}$. The time for the phase locking of the intermediate frequency is less than 1 ms. The frequency range of 24–40 GHz, is comparable to the frequency range of the already existing generator (36–37 GHz). The new generator has been put into regular operation for all three antennae arrays and allows up to 9 different preprogrammed frequencies and durations within a discharge. Duration and frequency are freely adjustable. The generator can be synchronized with the TEXTOR timing system which allows automatic frequency hopping with respect to the plasma start or any other preprogrammed time. Both generators are computer controlled and are operated from the control room during experiments.

The existing set–up allows now the measurement of poloidal rotation at three different positions. In Fig. 1 the different combinations are shown. Radial correlations are measured at the top and midplane I position. Midplane II position is use for poloidal correlations and toroidal correlations between either midplane II and midplane I or midplane II and the top position.

For the radial correlations one generator is operated at a fixed frequency whereas the second generator frequency is shifted in a staircase like way. In this way it is possible to obtain the radial correlation as function of the frequency difference respectively the difference of the cut off layers. In addition for constant ∇n_e and fixed Δf between both generators, implying a fixed radial separation, a large radial range can be probed by equally shifting the frequency of both generators.

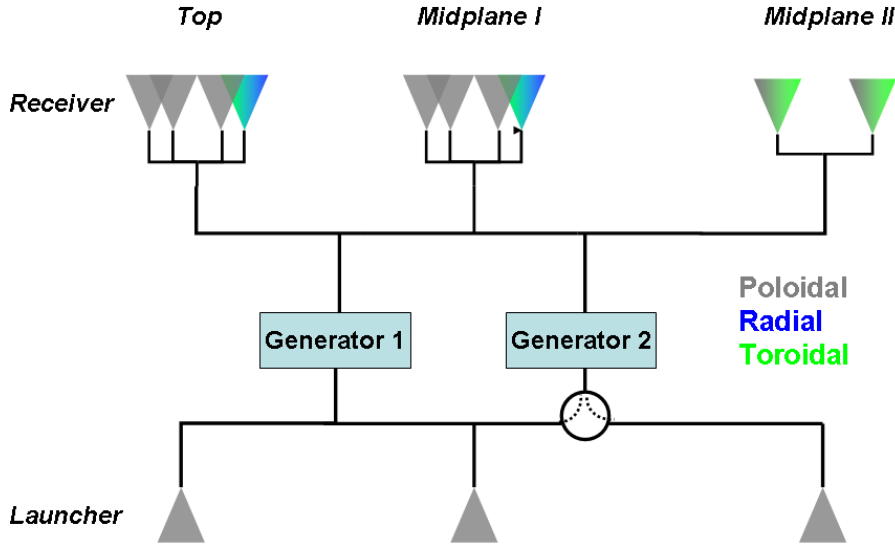


Figure 1: Color coded the different correlations at TEXTOR are shown. For radial correlations a fixed antennae in either top or midplane position is used

First Examples

First measurements are done with the aim to deduce the radial correlation length of density fluctuations at different poloidal positions and to investigate the radial correlation length of the geodesic acoustic mode (GAM).

Comparison of top and midplane radial correlations

In a first attempt ohmic discharges at $I_p = 400$ kA and $B_t = 1.9$ T are studied. The first generator was kept at $f_1 = 26$ GHz and the second one is operated from $f_2 = 24$ GHz to $f_2 = 30$ GHz in steps of 1 GHz. The radial range for the studies is $0.8 \leq r/a \leq 0.88$, where the density scale length increases from $L_n = 0.04$ to $L_n = 0.09$.

The interpretation of radial correlations is quite difficult and depends on the level of the phase fluctuations. If the level is too high multiple scattering of the probing wave can perturb the measurements. Following the discussion in [1], radial correlation measurements are possible as long as the phase spectrum shows significant deviations from a $1/f^2$ dependence. This is consistent with a complex amplitude spectrum showing coherent reflections. The important parameter controlling the shape of the spectra is the level of the phase fluctuation ($\sigma(\phi)$) or more convenient the related level of density fluctuations ($\delta n/n_c$). A similar criterium based on the level of $\delta n/n_c$ is also used by Gusakov and coworkers [2] who invent the following equation;

$$\gamma_s = \frac{\omega_0^2 l_c x_c(\omega_1)}{c^2} \frac{\delta n^2}{n_c^2} \ln\left(\frac{x_c(\omega_1)}{l_c}\right) \quad (1)$$

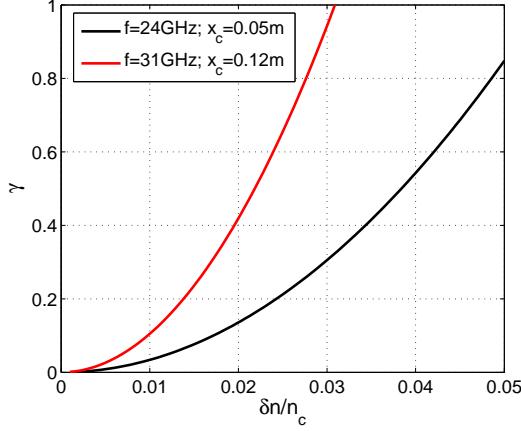


Figure 2: Calculation of γ_s as function of $\delta n/n_c$ with a fixed radial correlation length $l_c = 0.01$ m

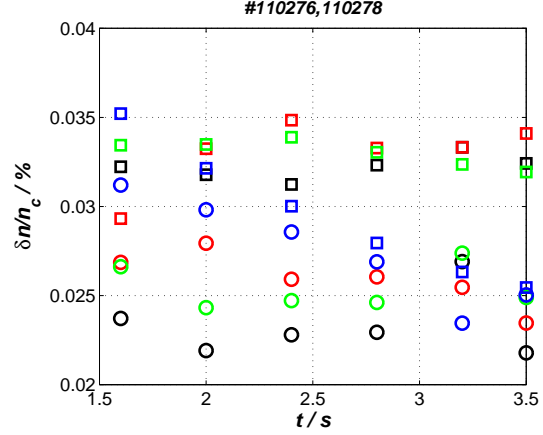


Figure 3: Phase fluctuation for top and mid-plane antennae. A clear increase in $\delta n/n_c$ for all antennae in the midplane is observed

to distinguish between linear and non linear scattering regime. In this equation x_c denotes the distance the wave travels in the plasma and $\delta n^2/n_c^2$ the squared density fluctuation level, $\omega_{0,1}$ denotes the probing frequencies and l_c the radial correlation length. In addition to the phase fluctuation γ_s depends on x_c . With increasing (x_c deeper in the plasma core) γ_s increases and compensates partly the effect of decreasing $\sigma(\phi)$. As long as $\gamma_s \ll 1$ (linear regime) turbulence properties as radial correlation length can be determined from the measurement. For two extreme conditions at TEXTOR γ_s is calculate and shown in fig. 2 as function of $deltan/n_c$. For the calculation $l_c = 0.01$ m is fixed. An increase of γ_s with the travelled distance to the cut off layer is seen in fig. 2. A part of the increase in γ_s will be reduced by the decrease of $deltan/n_c$ in the gradient region. To deduce $deltan/n_c$ for the analyzed discharges, $\sigma(\phi)$ is calculated separately for each single antennae of top and midplane respectively. According to the following equation:

$$\frac{\langle |\delta n|^2 \rangle^{1/2}}{n_c} \approx \sigma_\Phi \cdot \frac{\lambda_0}{4\pi \cdot 1.5 \cdot 2^{-1/4} \sqrt{L_n/l_c}} \quad (2)$$

the density fluctuation level is estimated (see fig. 3). Here λ_0 denotes the probing vacuum wavelength. The radial correlation length is approached by the relation $l_c = 1/2\lambda_\perp$, where $\lambda_\perp = 0.024$ m denotes the perpendicular wavelength which is estimated from cross correlation analysis of the three poloidally spaced antennae ($\Delta\theta = 0.025, 0.05, 0.075$ rad) operating at the same frequency. In fig. 3 the calculated $\delta n/n_c$ is shown. The different antenna are color coded. The \square symbols denote the midplane position and \circ the top position. For all antennae of the midplane array we observe an increase by 25 %, compared to the top array. The difference is attributed to the reduction in the local magnetic field B_t at the midplane, assuming that the

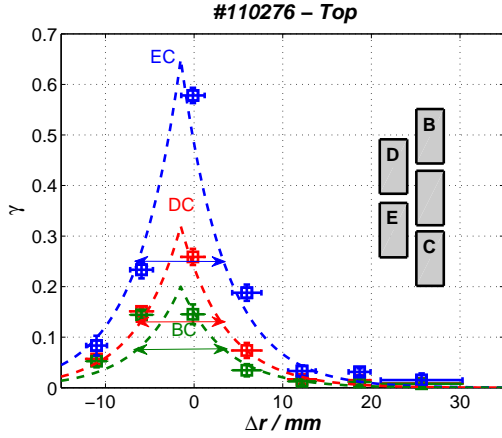


Figure 4: *Complex coherence as function of the Δr . The three different combination for top antennae yield the same l_c . A shift between the generator frequencies of $\Delta f \approx 400$ MHz is seen*

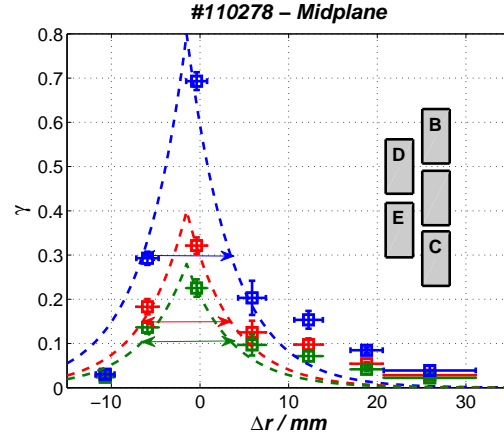


Figure 5: *Same as in fig. 4 but for midplane antennae. Note the increased coherency for $\Delta r > 5$ mm*

turbulence level scales with the Larmor radius. For the investigated ohmic discharge the relation $B_R \cdot \delta n/n_c = const$ is found for top and midplane array. Furthermore a decrease in $\delta n/n_c$ is observed for the channel with the increasing frequency (blue colored symbols) independent from top and midplane antennae array. Because of the temporal increasing frequency this channel shows that $\delta n/n_c$ decreases with decreasing radius. With the $\delta n/n_c$ from fig. 3 γ_s in fig. 2 is estimated. For the investigated radial range of $\delta n/n_c$ the condition $\gamma_s < 1$ is fulfilled. Therefore the analysis of l_c from the radial correlations for the top array is possible.

The mean coherence of the complex signal is calculated for the frequency range $70 \leq f \leq 100$ kHz, which denotes the frequency range of the quasi coherent mode. In fig. 4 the coherence is shown as function of the radial separation for the top antennae. The different colors denote the different poloidal spacing. With increasing poloidal distance between the antennae the coherence is decreasing. All three combinations can be described by the same exponential function. Assuming that the decay in the coherence is symmetric, a shift of the maximum in the coherence of $\Delta r = 2$ mm is found. For the plasma parameters under consideration this shift can be attributed to a systematic difference in the frequency of the generators of $\Delta f \approx 400$ MHz. The coherence for the two largest radial separations has nearly vanished. Taking the full width at $1/e$ level as a measure of the the radial correlation length, a value of $l_c = 11$ mm is obtained for all three combinations. The same analysis for the midplane antennae (see fig. 5) yields a similar dependency. However, for radial separations $\Delta r > 5$ mm an increased coherence level compared to the top antennae is observed. For $\Delta r \leq 5$ mm the values for top and midplane

antennae array are in good agreement. This is also seen by the $1/e$ level which is indicated by double arrows. In the authors opinion it shows that the level of $\sigma(\phi)$ is crucial for the estimation of l_c . In the case for the midplane antennae $\sigma(\phi) \approx 1.35$ rad which is close to $\pi/2$. This value is suggested by [3] as the threshold between the linear and nonlinear scattering regime. The fact that the deviation in the coherence of the complex amplitude is largest at large radial separations is observed also in the simulations by Blanco et al. [4]. However, it allows the determination of l_c even at the transition to the nonlinear regime, by restricting the range of radial separation. It should be noted here that the above discussion depends on the fact of the real measurement of l_c at the top array. No independent measurement of l_c is available to strengthen the statements made here.

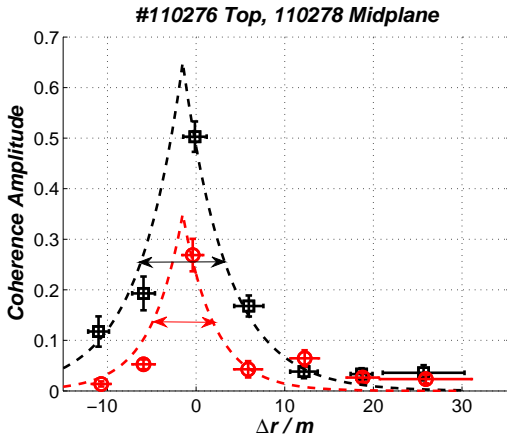


Figure 6: *Coherence of the amplitude estimated for the top (□) and midplane (○) antennae.*

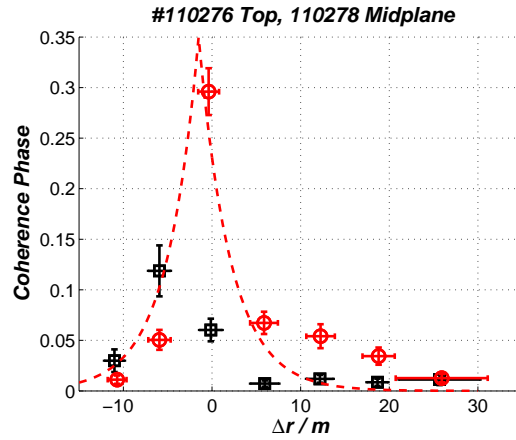


Figure 7: *Coherence of the phase estimated for top (□) and midplane (○) antennae.*

For the analyzed discharges the ratio between correlation length and the probing wavelength is in the order $0.97 \leq l_c/\lambda_0 \leq 1.3$ and $\gamma_s \approx 0.15$. According to the work by Blanco et al. [4] and for the mentioned parameters the amplitude should describe the correlation length better than the complex signal or the phase. Both, coherence of amplitude and phase are shown in figs. 6, 7 for top and midplane antennae array and the antennae combination with the shortest poloidal distance (EC). In the amplitude case top and midplane antennae show a similar picture. However the coherence is reduced by a factor of 2 and the correlation length is reduced to $l_c = 7$ mm for the midplane. The data for $\Delta r > 5$ mm are in both cases close to zero. Comparing the coherence calculated from the complex signal of the top antennae, combination EC, (fig. 4) with the one obtained from the amplitude (fig. 6), no difference is found. The same comparison for midplane antennae exhibits for $\Delta r > 5$ mm a significant reduction of the coherence. Both data sets can be approached by a similar fit. However the $1/e$ level (indicated by double arrows) for

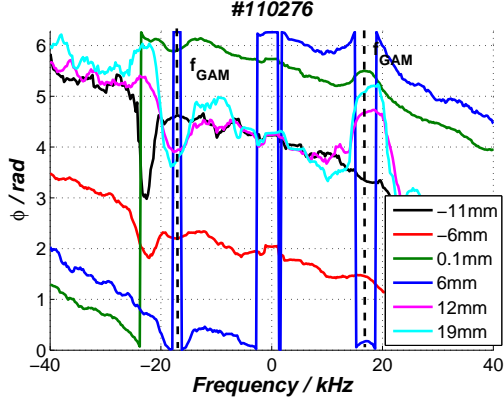


Figure 8: Cross phase as function of Δr . Dashed lines denote f_{GAM} .

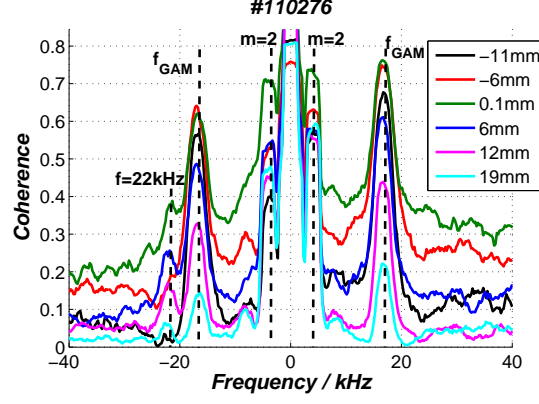


Figure 9: Coherence as function of Δr .

the midplane array is $\approx 20\%$ smaller than the one for the top array. The coherence of the phase (fig. 7) overestimates l_c in case of the midplane antennae and yields a strange result for the top antennae, due to a shifted maximum of $\Delta r = -5$ mm. Under assumption that l_c obtained from the top array is the real correlation length, the estimation of l_c from the coherence of the amplitude is more unambiguous than the coherence of the complex signal which is in agreement with the simulations obtained by [4].

Radial correlation of GAMs

The radial range under investigation shows also density fluctuations caused by GAMs in the top antennae signals. Information on GAMs you can find elsewhere [5, 6, 7]. With the existing set up the radial correlation length of the GAM induced density fluctuation is investigated. GAMs have a $m = 1$ structure which results in a large poloidal structure. They cover the frequency range $13 \leq f \leq 19$ kHz and are pronounced visible in at $\theta = 90^\circ$. The coherence (γ) and cross phase (ϕ) spectra are shown in figs. 8, 9, respectively. To reduce the noise level, averaging for the duration of each frequency step is applied. The slope in the cross phase spectrum for the ambient turbulence is constant for all radial positions. At f_{GAM} a deviation is visible for the smallest Δr . The deviation increases with increasing Δr and the maximum of the deviation shifts slightly to higher frequencies. The coherence spectrum shows beside the peak at f_{GAM} the $m = 2$ kink mode at $f = 4$ kHz. Furthermore a peak at $f = -22$ kHz becomes visible for $\Delta r > 0$. No shift in f_{GAM} is observed in the coherence spectrum. At the GAM frequency the coherence of the complex signal and cross phase are estimated for each radial position. The coherence at f_{GAM} is determined for all three combinations with $\theta = 0.025, 0.075$ and 0.1 rad. In fig. 10 γ is shown as function of the radial separation. The reference reflection layer is located at $r_c^{Ref}/a = 0.86$. Negative Δr means measurements with $r_c \leq r_c^{Ref}$. The radial error bar stems from averaging for the duration of a frequency step. For the points with $\Delta r 30$ mm a decrease

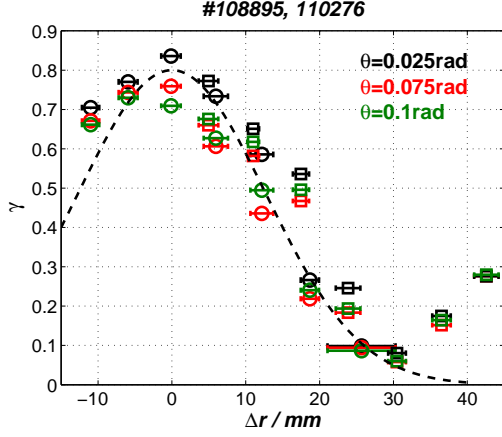


Figure 10: Coherence for two discharges, $\square = 108895$ and $\circ = 110276$. The different color codes denote different poloidal spacing. The black dashed line denotes an exponential fit.

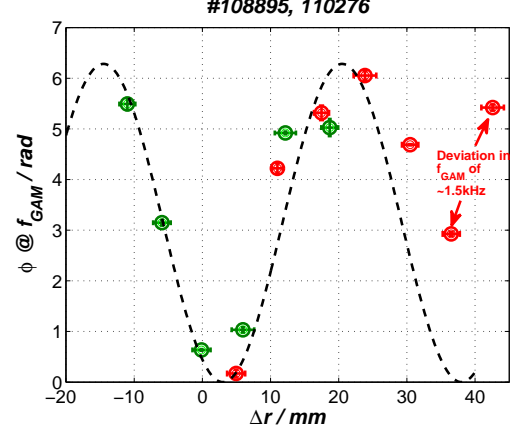


Figure 11: Cross phase ϕ estimated for two different discharges. The data can be approached by a sinusoidal fit (dashed line).

in the f_{GAM} of 1-1.5 kHz is observed. Therefore it is questionable if these data still belong to a GAM. The data can be approached in good agreement by an exponential function with a $1/e$ level of 18 mm.

Of interest is also the radial phase development. Therefore the cross phase at f_{GAM} is analyzed for all three combinations. In a first step the absolute cross phase is obtained. An offset between the different combinations is found. It is different for each antennae configuration (different $\Delta\theta$) but does not change with the variation of the reflection layer. After a correction for phase jumps the mean of all three combinations is calculated (see fig. 11). The different colors denote two different discharges probing different Δr . Despite the last two outer data points at $\Delta r = 36$ mm and $\Delta r = 43$ mm who deviate by more than 1.5 kHz from the GAM frequency, f_{GAM} is constant. In addition a shift of the minimum in ϕ by $\Delta r \approx 3$ mm is observed, which could be caused by a slight frequency difference of both generators. The data from both discharges can be approached by a sinusoidal function (dashed curve in fig. 11). The period of the sinusoidal function (black dashed line in fig.11) is $\lambda = 35$ mm. This results shows that hypothesis of 2 annular regions which are in anti phase is valid for the GAMs. Each annular region has a width of $\Delta r \approx 18$ mm and which is larger than the radial correlation length of the ambient turbulence.

For the estimation of the wave number the data from the cross phase measurement are taken. It confirms a large radial wavelength of GAMs as measured with probes at HL2A [8]. The radial wave number of the GAM amounts to $k_r^{GAM} = 2\pi/\lambda \approx 1.8 \text{ cm}^{-1}$.

Conclusions

The paper reports on the hardware extension of the reflectometer system at TEXTOR which consists of the installation of an additional toroidal antennae and a second generator. It enhances the measurement capabilities at TEXTOR, especially first observation of radial correlations at the midplane and at $\theta = 90^\circ$ antennae array have been performed.

The radial correlation measurements are used for the investigation of the radial properties of the ambient turbulence as well as for the radial wavelength of the geodesic acoustic mode. Regarding the ambient turbulence it could be demonstrated that in ohmic plasmas the estimation of radial coherence length at $\theta = 90^\circ$ is possible and yields the same correlation length for the complex amplitude as well as for amplitude and phase separately. Even at higher density fluctuation level as at the midplane array the results are meaningful. However, with increasing radial separation the coherence of the complex signal is increased, which yields an overestimation of the radial correlation length. In this case the coherence from the amplitude only, yields a non perturbed alternative for the correlation length estimation and which yields similar values as obtained at the top array.

The radial structure of the geodesic acoustic mode is analyzed in the coherence and the cross phase as well. The cross phase measurements proves the existence of two annular layers which are in anti phase and whose width is larger than the radial correlation length of the ambient turbulence. Using the wavelength estimation from the cross phase, GAMs show a large radial wavelength which yield $k_r^{GAM} \approx 1.8 \text{ cm}^{-1}$. This value is in agreement with an earlier measurement of HL2A.

References

- [1] R. Nazikian and E. Mazzucato. *Rev. Sci. Instrum.*, 1:392–398, 1995.
- [2] E.Z. Gusakov and A.Yu. Popov. *Plasma Phys. Control. Fusion*, 44:2327–2337, 2002.
- [3] E. Gusakov et al. In *Proc. 9th Intl. Reflectometry Workshop - IRW9 (Lisboa, May 2009)*, IPFN Report, 2009.
- [4] E. Blanco et al. In *Proc. 9th Intl. Reflectometry Workshop - IRW9 (Lisboa, May 2009)*, IPFN Report, 2009.
- [5] G.D. Conway et al. *Plasma Phys. Control. Fusion*, 47:1165–1185, 2005.
- [6] A. Krämer-Flecken et al. *Nucl. Fusion*, 46:S730–S742, 2006.
- [7] A. Krämer-Flecken et al. *Plasma Phys. Control. Fusion*, 51:015001, 2009.

[8] T. Lan et al. *Plasma Phys. Control. Fusion*, 50:045002, 2008.